

Role of nuclear dissipation and entrance channel mass asymmetry in pre-scission neutron multiplicity enhancement in fusion-fission reactions

Hardev Singh,¹ K. S. Golda,² Santanu Pal,³ Ranjeet,² Rohit Sandal,¹ Bivash R. Behera,¹ Gulzar Singh,¹ Akhil Jhingan,² R. P. Singh,² P. Sugathan,² M. B. Chatterjee,² S. K. Datta,² Ajay Kumar,⁴ G. Viesti,⁵ and I. M. Govil¹

¹*Department of Physics, Panjab University, Chandigarh 160014, India*

²*Inter University Accelerator Centre, New Delhi 110067, India*

³*Variable Energy Cyclotron Centre, 1/AF, Bidhan Nagar, Kolkata 700064, India*

⁴*Department of Physics, Banaras Hindu University, Varanasi 221005, India*

⁵*Dipartimento di Fisica and Sezione INFN Padova, I-35131 Padova, Italy*

(Received 13 June 2008; published 28 August 2008)

Pre-scission neutron multiplicities are measured for $^{12}\text{C} + ^{204}\text{Pb}$ and $^{19}\text{F} + ^{197}\text{Au}$ reactions at laboratory energies of 75–95 MeV for the ^{12}C beam and 98–118 MeV for the ^{19}F beam. The chosen projectile-target combinations in the present study lie on either side of the Businaro-Gallone mass asymmetry (α_{BG}) and populate the ^{216}Ra compound nucleus. The dissipation strength is deduced after comparing the experimentally measured neutron yield with the statistical model predictions which contains the nuclear viscosity as a free parameter. Present results demonstrate the combined effects of entrance channel mass asymmetry and the dissipative property of nuclear matter on the pre-scission neutron multiplicity in fusion-fission reactions.

DOI: [10.1103/PhysRevC.78.024609](https://doi.org/10.1103/PhysRevC.78.024609)

PACS number(s): 25.70.Jj, 25.70.Gh, 24.10.Pa

I. INTRODUCTION

The dynamics of fusion-fission processes in nucleus-nucleus collisions has been extensively investigated, both experimentally and theoretically, in recent years. The experimental probes for these studies are mainly the pre-scission multiplicities of light particles including photons and evaporation residue cross sections. Neutrons emitted at the pre-scission stage are detected in most of the experiments [1–5], though measurements of pre-scission multiplicities of light charged particles [6,7] and high-energy γ rays [8,9] have also been reported. The measured pre-scission multiplicities of different light species are found to be substantially higher than those predicted by the standard statistical model of fission [10]. A dissipative dynamical model, originally proposed by Kramers [11], is now considered essential to describe fission of nuclei at high excitations.

The emission of pre-scission neutrons can take place at different stages of a fusion-fission reaction, starting from the formation of a compound nucleus (CN) till it reaches the scission configuration. Initially, the dinuclear system in the entrance channel requires a time interval (t_{form}) in order to form a fully equilibrated CN. Due to fast energy equilibration in the di-nuclear system [3], neutron evaporation can take place during t_{form} and it would contribute to the measured pre-scission multiplicity. After the CN is formed, its dynamical evolution can be considered as a quasistationary diffusion process over the fission barrier. Most of the pre-scission neutrons are emitted during this stage. Beyond the saddle point, neutron emission from the CN can still continue till it reaches the scission point and this would make an additional contribution to the multiplicity of pre-scission neutrons.

In heavy ion induced fusion-fission reactions, it is possible to create the same CN at the same excitation energy through different entrance channels by choosing proper combinations of the target and projectile nuclei and appropriate beam

energies of the projectiles. For such compound nuclei formed through different entrance channels, the average number of pre-scission neutrons emitted after formation of the CN are expected to be the same. However, the number of neutrons emitted during the formation time t_{form} in different reactions could be different depending upon the dynamics of the respective entrance channels. It is well established [3,12,13] that entrance channel mass asymmetry $\alpha = (A_t - A_p)/(A_t + A_p)$ plays a major role in the dynamical evolution of a dinuclear system leading to the formation of a CN and the fusion path followed by the composite system is quite different for the two cases of $\alpha < \alpha_{\text{BG}}$ and $\alpha > \alpha_{\text{BG}}$, where α_{BG} is the critical Businaro-Gallone mass asymmetry [14–16]. The multiplicity of pre-scission neutrons would therefore be expected to depend upon the entrance channel mass asymmetry.

The quasifission process is known [13,17] to take place accompanying the fusion-fission process in a number of heavy ion induced reactions depending upon the projectile plus target combination. In quasifission, the dinuclear complex formed after capture of a projectile by a target separates into two fragments before full mass equilibration is established. Energy equilibration however takes place in quasifission and neutrons can be evaporated from the dinuclear complex. The average life-time of a partially equilibrated dinuclear complex is expected to be smaller than that of a fully equilibrated compound nucleus. Consequently, the average number of neutrons emitted in quasifission events would be smaller than that from the compound nucleus. Thus occurrence of quasifission events can affect the multiplicity of pre-scission neutrons.

We have assumed in the foregoing discussions that the spin distributions of compound nuclei formed through different entrance channels are similar. However, a CN may be formed at the same excitation energy but with different spin distributions when the difference between the Q-values of two entrance

channels is large. As the average lifetime of a CN decreases with increase of spin, more neutrons will be emitted from a CN with a smaller spin than from the one with a larger spin though both of them are formed at the same excitation energy. Therefore, the compound nuclear spin distribution can also leave its signature on the multiplicity of pre-scission neutrons.

Entrance channel effects on pre-scission neutron multiplicities have been experimentally observed [3,18] in a few measurements. In an earlier experiment [18], we have observed different pre-scission neutron yields for the two entrance channels ($^{16}\text{O} + ^{181}\text{Ta}$ and $^{19}\text{F} + ^{178}\text{Hf}$) lying on either side of the Businaro-Gallone point and populating the ^{197}Tl compound nucleus at the same excitation energies with similar spin distributions. It was shown in this work that the entrance channel dependence of pre-scission neutron yield can be attributed to the longer formation time of the more symmetric system and this was reflected into the magnitude of the dissipation strength required to fit the data.

In the present work, the multiplicity of pre-scission neutrons is measured for the systems $^{12}\text{C} + ^{204}\text{Pb}$ ($\alpha = 0.888$) and $^{19}\text{F} + ^{197}\text{Au}$ ($\alpha = 0.824$) lying on the two sides of the Businaro-Gallone point ($\alpha_{\text{BG}} = 0.849$). The measurements are made at different laboratory energies. At three energies, the compound nucleus ^{216}Ra is formed at the same excitation energies in the two reactions. The present systems are distinguished by the fact that they populate the CN with different spin distributions at the same excitation energies. Further, quasifission has been observed earlier in the $^{19}\text{F} + ^{197}\text{Au}$ system but not in the $^{12}\text{C} + ^{204}\text{Pb}$ system [13]. Therefore, we shall be able to study the combined effect of entrance channel (formation time effect plus quasifission) dependence and CN spin distribution on the multiplicity of pre-scission neutrons. To this end, we shall make a detailed comparison of the measured values with the statistical model predictions.

II. EXPERIMENTAL DETAILS

The experiment was performed using pulsed beams of ^{12}C ($E_{\text{lab}} = 75, 79, 83, 87, 91, \text{ and } 95 \text{ MeV}$) and ^{19}F ($E_{\text{lab}} = 98, 102, 106, 110, \text{ and } 118 \text{ MeV}$) obtained from 15UD Pelletron of Inter University Accelerator Centre (IUAC), New Delhi. A self-supporting ^{197}Au target of $250 \mu\text{g}/\text{cm}^2$ thickness and ^{204}Pb having thickness of $200 \mu\text{g}/\text{cm}^2$ sandwiched between carbon foils were used in the experiment. Two large area ($20 \text{ cm} \times 10 \text{ cm}$) position sensitive multiwire proportional counters (MWPC) were placed at the folding angle for symmetric fission. Detectors were placed on movable arms on both sides of the beam at distance of 63.5 cm and 51.5 cm respectively from the target. The position of one detector placed at 63.5 cm was fixed at 90° with respect to the beam direction and the position of other detector was adjusted according to the folding angle depending upon the beam energies and projectile-target combination.

The neutrons were detected in coincidence with fission events by four neutron detectors, which consisted of $12.7 \text{ cm dia} \times 12.7 \text{ cm thick}$ organic liquid scintillator cells (BC501) coupled to 12.7 cm XP4512B Photomultiplier tubes and were placed outside the scattering chamber at a distance of

100 cm from the target. Thin flanges of 3 mm stainless steel (SS) were used with the scattering chamber in order to minimize neutron scattering. These detectors were placed at angles of $30^\circ, 60^\circ, 90^\circ, \text{ and } 120^\circ$ with respect to the beam direction. The neutron detector array threshold was kept at about 120 keVee by calibrating it with standard γ -sources (^{137}Cs and ^{60}Co) [19]. Two silicon surface barrier detectors were used at $\pm 11^\circ$ for beam flux normalization purpose. The time of flight of neutrons was obtained with reference to the fission fragments detected in either of the gas detector. The details of the experimental setup can be found at [18]. In order to keep the background in TOF spectra at minimum level, the beam dump was kept at 3 m from the target and was well shielded with layers of lead and borated paraffin. A discrimination between neutrons and gammas was made by using pulse shape discrimination (PSD) based on zero cross technique and TOF. The dual channel PSD modules having built in shaping amplifier, constant fraction discriminator (CFD), PSD and time to amplitude converter (TAC) were developed at IUAC, New Delhi [20]. Data were also taken with a blank target to estimate the level of background in the neutron spectra and it was found to be negligible. The TOF of neutrons was converted into neutron energy by considering the prompt γ peak in TOF spectrum as the time reference. The efficiency correction for the neutron detectors was done using Monte Carlo computer code MODEFF [21]. The Monte Carlo calculations, in turn, were verified by measuring the relative efficiency of the detector using a ^{252}Cf spontaneous fission source [22].

III. DATA ANALYSIS

Pre- and post-scission neutron multiplicities were obtained by fitting the observed neutron energy spectra with three moving source evaporation components (pre-scission emission is assumed to be from CN and post-scission from two fully accelerated fission fragments) using the Watt expression [23]. The neutron emission from these moving sources was assumed to be isotropic in their respective rest frames. Thus, the measured double differential neutron multiplicities are given as

$$\frac{d^2 M_n}{dE_n d\Omega_n} = \sum_{i=1}^3 \frac{M_{n_i} \sqrt{E_n}}{2(\pi T_i)^{3/2}} \exp \left[-\frac{E_n - 2\sqrt{E_n E_i / A_i} \cos \theta_i + E_i / A_i}{T_i} \right]. \quad (1)$$

Here, E_n is the laboratory energy of the neutron and E_i, T_i, M_{n_i} represent energy, temperature, and multiplicity, respectively, of each neutron emission source. A_i is mass of each neutron source and θ_i represents the relative angle between the neutron direction and the source direction. The folding angles were obtained from the Viola [24] systematics for symmetric fission. The angular acceptance of the neutron detectors and the fission detectors were taken into account in the fitting procedure. Figures 1 and 2 shows the fits to the double differential neutron multiplicity spectra at various angles for both the

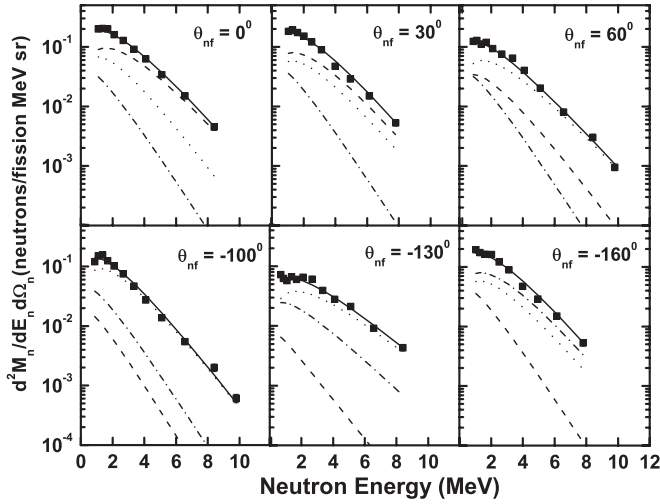


FIG. 1. Neutron multiplicity spectra (filled squares) for the $^{12}\text{C} + ^{204}\text{Pb}$ reaction at $E_{\text{lab}} = 90$ MeV along with the fits for the pre-scission (dotted curve) and the post-scission from fragment 1 (dashed curve) and fragment 2 (dot dashed curve). The solid curve represents the total contribution.

reactions. The post-scission multiplicity and the temperatures were assumed to be the same for both the fission fragments.

The observed pre-scission neutron multiplicities for both the reactions are shown in Fig. 3. The pre-scission neutron multiplicity is found to be higher for the system with entrance channel mass asymmetry $\alpha < \alpha_{\text{BG}}$ ($^{19}\text{F} + ^{197}\text{Au}$) as compared to the system lying on the other side, i.e., $\alpha > \alpha_{\text{BG}}$ ($^{12}\text{C} + ^{204}\text{Pb}$). This difference in multiplicities increases with the excitation energy of the CN.

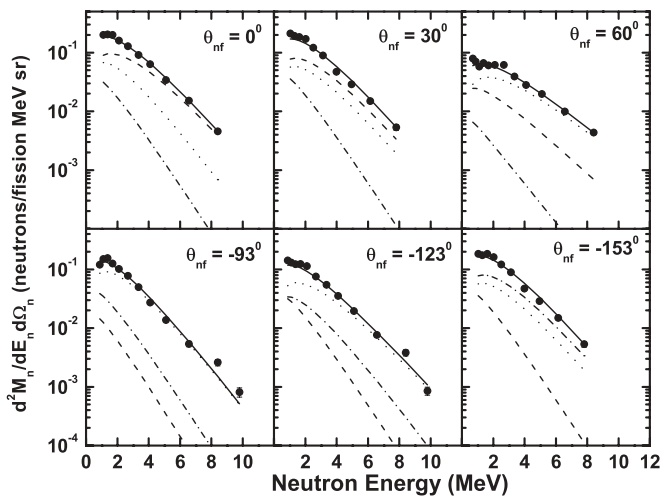


FIG. 2. Neutron multiplicity spectra (filled circles) for $^{19}\text{F} + ^{197}\text{Au}$ at $E_{\text{lab}} = 102$ MeV along with the fits for the pre-scission (dotted curve) and the post-scission from fragment 1 (dashed curve) and fragment 2 (dot dashed curve). The solid curve represents the total contribution.

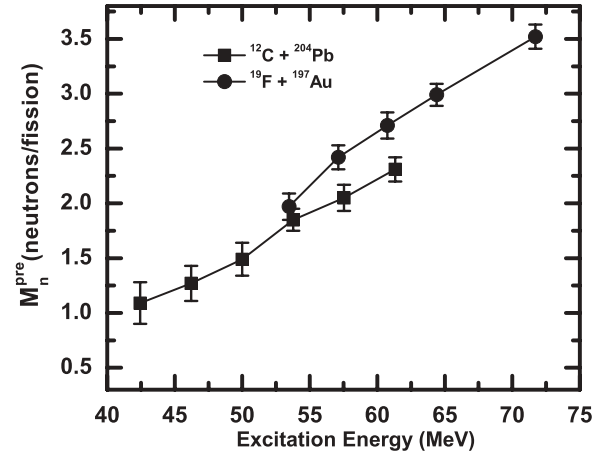


FIG. 3. Pre-scission neutron multiplicities from $^{12}\text{C} + ^{204}\text{Pb}$ (solid squares) and $^{19}\text{F} + ^{197}\text{Au}$ (solid circles) reactions. Lines are drawn to guide the eye.

IV. STATISTICAL MODEL ANALYSIS

The experimental neutron multiplicities were compared with the statistical model predictions for the decay of a CN. Emission of neutrons, protons, alphas, and GDR γ 's were considered as the decay channels of the CN in addition to fission in the present calculation. The neutron and GDR γ partial widths were obtained from the Weisskopf formula [25] while the fission width was calculated using the Kramers modified Bohr-Wheeler expression [11],

$$\Gamma_f^{\text{Kramers}} = \Gamma_f^{\text{BW}} [(1 + \gamma^2)^{1/2} - \gamma], \quad (2)$$

where γ represents the strength of nuclear dissipation and was treated as an adjustable parameter in the calculation. We may remark at this point that though γ is introduced in the present calculation as the strength of the dissipative force in the fission dynamics of the CN, its value obtained from fitting the experimental data has to account for the total number of neutrons emitted before fission including those emitted during the formation time (t_{form}) of the CN as well as those from quasifission. This point will be discussed further while comparing statistical model results with experimental data. The Bohr-Wheeler fission width was calculated using the fission barrier obtained from the finite range liquid drop model for the nuclear potential [26]. A dynamical fission width was subsequently obtained as

$$\Gamma_f(t) = [1 - \exp(-2.3t/\tau_f)] \Gamma_f^{\text{Kramers}}, \quad (3)$$

where τ_f accounts for the build up or transient time required for the fission width to reach its stationary value. The value of τ_f was taken from Refs. [27,28]. The level density parameter used in the present study was taken from the work of Ignatyuk *et al.* [29,30], who proposed a form which includes the shell structure effects at low excitations. Using the above partial widths, the time evolution of a CN was followed in the statistical model code [31,32] till either fission occurred or an evaporation residue was formed. In the case of a fission event, the number of neutrons emitted during saddle-to-scission transition was also included as pre-scission neutrons [33]. The multiplicity of neutrons emitted from the

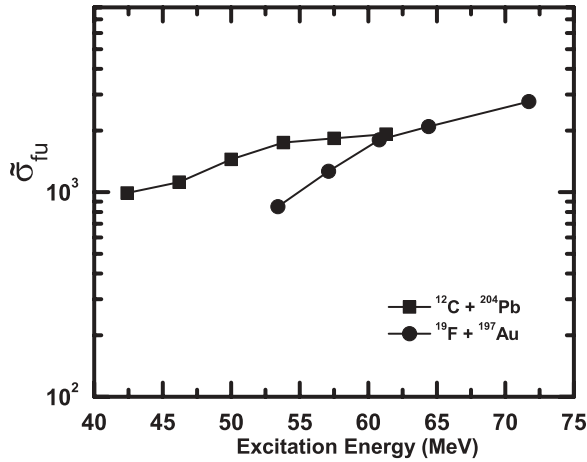


FIG. 4. Reduced fusion cross section (dimensionless, see text) for the two reactions. Lines are drawn to guide the eye.

fission fragments (post-scission neutrons) was also calculated assuming a symmetric fission.

The spin distribution of the CN was assumed to follow the usual Fermi distribution

$$\sigma(l) = \frac{\pi}{k^2} \frac{2l + 1}{1 + \exp\left(\frac{l - l_c}{\delta l}\right)}, \quad (4)$$

the parameters (l_c and δl) of which were fixed by fitting the experimental fusion cross sections [17,34]. The experimental fusion cross sections however show an interesting trend which throws light on the spin distributions in the compound nuclei populated through the two entrance channels. To illustrate this point, the excitation functions of the experimental reduced fusion cross sections, $\tilde{\sigma}_{fu}(E) = \sigma_{fu}(E)/\pi\lambda^2$, where, λ is the reduced de Broglie wavelength of the entrance channel, for the two reactions, $^{12}\text{C} + ^{204}\text{Pb}$ and $^{19}\text{F} + ^{197}\text{Au}$, are shown in Fig. 4. It is noted immediately that the reduced fusion cross sections are smaller for $^{19}\text{F} + ^{197}\text{Au}$ than $^{12}\text{C} + ^{204}\text{Pb}$. Specifically, the difference is largest at 53 MeV of excitation energy (E_x) and becomes smaller at higher E_x . The above difference in fusion cross sections essentially arises due to the large difference in the Q -values of the two entrance channels ($Q = -28.4$ MeV for $^{12}\text{C} + ^{204}\text{Pb}$ and -35.9 MeV for $^{19}\text{F} + ^{197}\text{Au}$ systems). Consequently, the critical angular momenta l_c are smaller for $^{19}\text{F} + ^{197}\text{Au}$ (28.2, 34.7, and 41.6 in \hbar unit) than those for $^{12}\text{C} + ^{204}\text{Pb}$ (41.0, 42.0 and 43.0 in \hbar unit) at excitation energies of 53, 57, and 61 MeV, respectively. In Fig. 5, the calculated pre-scission neutron multiplicity (M^{pre}) for different values of γ are shown along with the experimental data. We note here that for all values of γ , the calculated M^{pre} at $E_x = 53$ MeV is significantly larger for $^{19}\text{F} + ^{197}\text{Au}$ than for $^{12}\text{C} + ^{204}\text{Pb}$. However, they become almost equal at $E_x = 61$ MeV. The difference in compound nuclear spin distribution is thus adequately reflected in the calculated values of M^{pre} . The statistical model results would therefore serve as a baseline to assess the entrance channel effects in order to fit the experimental data.

We have further calculated the number of neutrons emitted during saddle-to-scission transition and the results are shown in Fig. 6. We find that such neutrons account for a small fraction

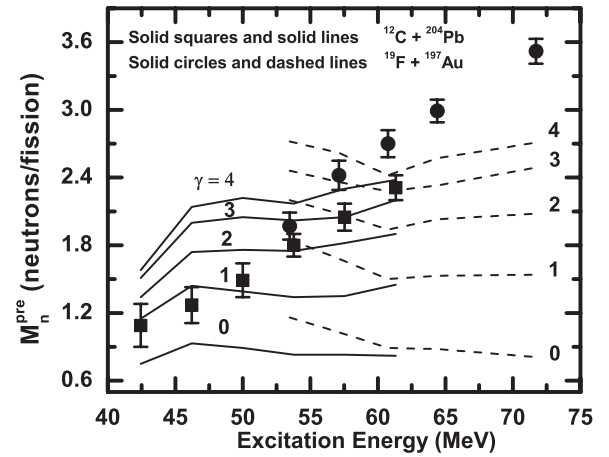


FIG. 5. Experimental pre-scission neutron multiplicities along with the statistical model calculation results.

of the total pre-scission neutron multiplicity. Therefore, the difference in the calculated M^{pre} values between the two systems can be solely attributed to the different fission barriers encountered in the two systems due to different spin distributions.

We shall now compare the experimental M^{pre} values with the statistical model results. We immediately note that the experimental and theoretical values present different trends in the overlap region of excitation energies between the two systems. In fact, this difference reflects the entrance channel dependence of the multiplicity of pre-scission neutrons for the present systems. Qualitatively, neutrons emitted (M^{form}) during the formation time t_{form} should make an additional contribution to the statistical model predictions since neutron emission in the statistical model is considered only after a CN has been formed. On the other hand, the number of neutrons emitted (M^{qf}) in quasifission events is expected to be smaller than the statistical model prediction since the dinuclear complex in quasifission has a shorter life time than the fully equilibrated CN. Quasifission events would therefore reduce the statistical model prediction of M^{pre} . In the present study, the two entrance channels lie on the two sides of

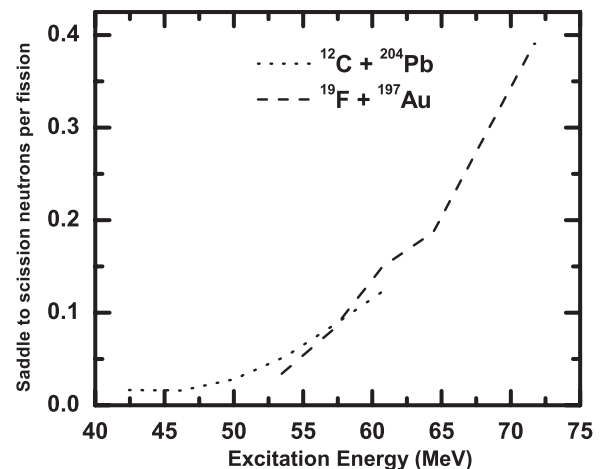


FIG. 6. Neutron yield from saddle-to-scission transition.

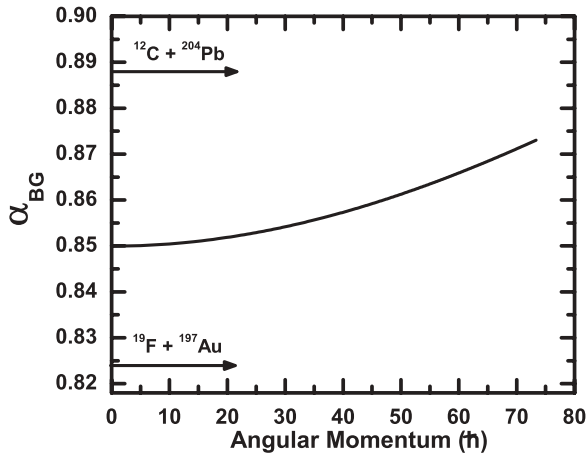


FIG. 7. Angular momentum dependence of Businaro-Gallone point for ^{216}Ra compound system.

the Businaro-Gallone point for all values of CN spin under consideration [16] as shown in Fig. 7. Therefore, the entrance channel dynamics would be quite different for the two systems. While the projectile nucleus will be swallowed by the target nucleus to form the CN in the less symmetric $^{12}\text{C} + ^{204}\text{Pb}$ system, a considerable amount of mass flow will take place from the target nucleus to the projectile nucleus in order to form the CN for the more symmetric $^{19}\text{F} + ^{197}\text{Au}$ system. Consequently, the t_{form} would be larger for $^{19}\text{F} + ^{197}\text{Au}$ than the $^{12}\text{C} + ^{204}\text{Pb}$ system. Hence M^{form} would also be larger for the more symmetric ($^{19}\text{F} + ^{197}\text{Au}$) system as compared to the other system. Further, it has been reported earlier by Berriman *et al.* [13], that a considerable amount of the entrance channel flux goes into quasifission for the $^{19}\text{F} + ^{197}\text{Au}$ system though none has been observed in the $^{12}\text{C} + ^{204}\text{Pb}$ system. This suggests that the average number of evaporated neutrons would be depleted only for the $^{19}\text{F} + ^{197}\text{Au}$ system due to quasifission. It thus becomes evident that M^{form} and M^{qf} together should account for the difference between the statistical model predictions and the experimental pre-scission neutron multiplicities. However, detailed calculations of entrance channel dynamics would be required in order to make further quantitative assessment of M^{form} and M^{qf} .

We shall now present in Fig. 8 the γ values that reproduce the experimental M^{pre} at each initial excitation energy for the two systems. The statistical error associated with an experimental multiplicity gives rise to an error on the corresponding fitted values of γ and it is also shown in this figure. It is observed that γ increases with the initial excitation energy for both the systems and the rate of increase is higher for the more symmetric system. However, the γ values obtained from fitting the experimental data here have to account for not only the fission hindrance of the CN but also the additional neutrons due to entrance channel effects. Specifically, we observe that the excitation energy dependence of γ for the two systems are significantly different in the range of $E_x = 53\text{--}61$ MeV. Thus the differences in entrance channel dynamics and CN spin distributions essentially give rise to the different rates of excitation energy dependence of γ . It may be remarked at this point that microscopic theories such as two-body viscosity can

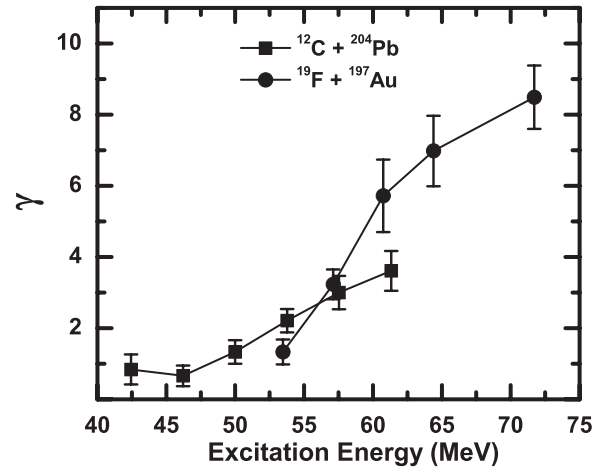


FIG. 8. Excitation energy dependence of dissipation strength. Lines are drawn to guide the eye.

give rise to an excitation dependence of γ . It is therefore not the initial excitation energy dependence of γ but the difference in the excitation energy dependence between the two systems that is considered here as a signature of entrance channel dynamics and CN spin distributions.

Lastly, we shall discuss the excitation energy dependence of the post-scission neutrons (M^{post}) emitted by the fission fragments. Figure 9 shows the experimental values along with the statistical model results. We first observe in this plot that the experimental M^{post} for both the systems is fairly independent of the excitation energy of the CN. This indicates that the excitation energy available to the fission fragments is nearly the same for all excitation energies of the CN, the balance being carried away by the emitted particles before scission. The γ dependence of the calculated values of M^{post} arises because the available excitation energy of the fission fragments is determined by the number of pre-scission neutrons. Consequently, the γ dependence of M^{post} has a complementary nature to that of M^{pre} over the entire range of excitation energy for both the systems.

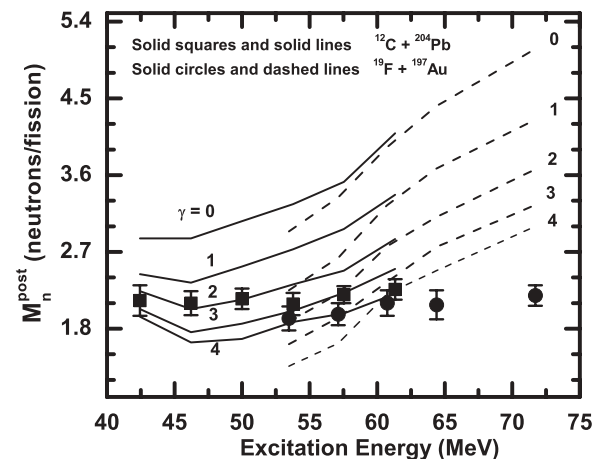


FIG. 9. Experimental post-scission neutron multiplicities along with the statistical model calculation results.

V. SUMMARY AND CONCLUSIONS

The multiplicities of pre- and post-scission neutrons emitted in the fission of ^{216}Ra compound nucleus have been measured using two different entrance channels ($^{12}\text{C} + ^{204}\text{Pb}$ and $^{19}\text{F} + ^{197}\text{Au}$) which lie on either side of the Businaro-Gallone point. The CN was formed at a number of excitation energies, three of which (53, 57, and 61 MeV) were the same for both the entrance channels. The measured pre-scission multiplicity in the $^{19}\text{F} + ^{197}\text{Au}$ system was found to be higher than that from the $^{12}\text{C} + ^{204}\text{Pb}$ reaction at the same excitation energies of the CN. The difference in the M^{pre} values between the two systems was attributed to the compound nuclear spin distribution and the entrance channel dynamics comprising of the formation time emission and quasifission. Comparison of experimental values with statistical model predictions showed significant contributions from the entrance channel effects. Consequently, a stronger excitation energy dependence of the dissipation strength (γ) was required to fit the experimental data for the

$^{19}\text{F} + ^{197}\text{Au}$ compared to that of the $^{12}\text{C} + ^{204}\text{Pb}$ reaction. The present study thus demonstrates the sensitivity of pre-scission neutron multiplicity to entrance channel dynamics including quasifission.

ACKNOWLEDGMENTS

We gratefully acknowledge the useful discussions with Professor V. S. Ramamurthy on this manuscript. The help received from Mr. S. R. Abhilash for the target fabrication and Mr. P. Barua during the experiment is acknowledged with thanks. We are also thankful to the accelerator crew of IUAC for providing good quality pulsed beams as per the requirement. We would like to thank Department of Science and Technology (DST), New Delhi and the Council of Scientific and Industrial Research (CSIR), New Delhi, for financial support to carry out this work.

-
- [1] H. Rossner, D. Hilscher, D. J. Hinde, B. Gebauer, M. Lehmann, and M. Wilpert, *Phys. Rev. C* **40**, 2629 (1989).
- [2] D. J. Hinde, D. Hilscher, H. Rossner, B. Gebauer, M. Lehmann, and M. Wilpert, *Phys. Rev. C* **45**, 1229 (1992).
- [3] A. Saxena, A. Chatterjee, R. K. Choudhury, S. S. Kapoor, and D. M. Nadkarni, *Phys. Rev. C* **49**, 932 (1994).
- [4] D. Hilscher, H. Rossner, B. Cramer, U. Jahnke, M. Lehmann, E. Schwinn, M. Wilpert, T. Wilpert, H. Frobeen, E. Mordhorst *et al.*, *Phys. Rev. Lett.* **62**, 1099 (1989).
- [5] J. Cabrera, T. Keutgen, Y. E. Masri, C. Dufauquez, V. Roberfroid, I. Tilquin, J. V. Mol, R. Regimbart, R. J. Charity, J. B. Natowitz *et al.*, *Phys. Rev. C* **68**, 034613 (2003).
- [6] J. P. Lestone, *Phys. Rev. Lett.* **70**, 2245 (1993).
- [7] K. Ramachandran, A. Chatterjee, A. Navin, K. Mahata, A. Shrivastava, V. Tripathy, S. Kailas, V. Nanal, R. G. Pillay, A. Saxena *et al.*, *Phys. Rev. C* **73**, 064609 (2006).
- [8] I. Diószegi, N. P. Shaw, I. Mazumdar, A. Hatzikoutelis, and P. Paul, *Phys. Rev. C* **61**, 024613 (2000).
- [9] I. Diószegi, N. P. Shaw, A. Bracco, F. Camera, S. Tettoni, M. Mattiuzzi, and P. Paul, *Phys. Rev. C* **63**, 014611 (2000).
- [10] N. Bohr and J. A. Wheeler, *Phys. Rev.* **56**, 426 (1939).
- [11] H. A. Kramers, *Physica (Amsterdam)* **7**, 284 (1940).
- [12] V. S. Ramamurthy, S. S. Kapoor, R. K. Choudhury, A. Saxena, D. M. Nadkarni, A. K. Mohanty, B. K. Nayak, S. V. Sastry, S. Kailas, A. Chatterjee *et al.*, *Phys. Rev. Lett.* **65**, 25 (1990).
- [13] A. C. Berriman, D. J. Hinde, M. Dasgupta, C. R. Morton, R. D. Butt, and J. O. Newton, *Nature (London)* **413**, 144 (2001).
- [14] U. L. Businaro and S. Gallone, *Nuovo Cimento* **1**, 629 (1955).
- [15] U. L. Businaro and S. Gallone, *Nuovo Cimento* **5**, 315 (1957).
- [16] M. Abe, KEK Report No. 86-26, KEK TH-28 (1986).
- [17] R. N. Sagaidak, G. N. Kniajeva, I. M. Itkis, N. A. Kondratiev, E. M. Kozulin, I. V. Pokrovsky, A. I. Svirikhin, V. M. Voskressensky, A. V. Yerein, L. Corradi *et al.*, *Phys. Rev. C* **68**, 014603 (2003).
- [18] H. Singh, A. Kumar, B. R. Behera, I. M. Govil, K. S. Golda, P. Kumar, A. Jhingal, R. P. Singh, P. Sugathan, M. Chatterjee *et al.*, *Phys. Rev. C* **76**, 044610 (2007).
- [19] T. G. Masterson, *Nucl. Instrum. Methods* **88**, 61 (1970).
- [20] S. Venkataraman, A. Gupta, Golda K. S., H. Singh, and R. K. Bhowmik, IUAC technical report IUAC/TR/SV/2006-2007/02.
- [21] R. A. Cecil, B. D. Anderson, and R. Madey, *Nucl. Instrum. Methods* **161**, 439 (1979).
- [22] K. S. Golda, H. Singh, R. P. Singh, S. K. Datta, and R. K. Bhowmik, National Symposium on Nuclear Physics, Vol. 50 (2005), p. 445.
- [23] D. Hilscher, J. R. Birkelund, A. D. Hoover, W. U. Schroder, W. W. Wilcke, J. R. Huizenga, A. C. Mignerey, K. L. Wolf, H. F. Breuer, and V. E. Viola, *Phys. Rev. C* **20**, 576 (1979).
- [24] V. E. Viola, K. Kwiatkowski, and M. Walker, *Phys. Rev. C* **31**, 1550 (1985).
- [25] P. Frobrich and I. I. Gontchar, *Phys. Rep.* **292**, 131 (1998).
- [26] A. J. Sierk, *Phys. Rev. C* **33**, 2039 (1986).
- [27] P. Grangé, S. Hassani, H. A. Weidenmuller, A. Gavron, J. R. Nix, and A. J. Sierk, *Phys. Rev. C* **34**, 209 (1986).
- [28] K. H. Bhatt, P. Grangé, and B. Hiller, *Phys. Rev. C* **33**, 954 (1986).
- [29] A. V. Ignatyuk, M. G. Itkis, V. N. Okolovich, G. N. Smirenkin, and A. Tishin, *Yad. Fiz.* **21**, 485 (1975).
- [30] A. V. Ignatyuk, M. G. Itkis, V. N. Okolovich, G. N. Smirenkin, and A. Tishin, *Sov. J. Nucl. Phys.* **21**, 255 (1975).
- [31] G. Chaudhuri and S. Pal, *Phys. Rev. C* **63**, 064603 (2001).
- [32] G. Chaudhuri and S. Pal, *Phys. Rev. C* **65**, 054612 (2002).
- [33] D. J. Hofman, B. B. Back, and P. Paul, *Phys. Rev. C* **51**, 2597 (1995).
- [34] R. Tripathi, K. Sudarshan, S. Sodaye, A. V. R. Reddy, K. Mahata, and A. Goswami, *Phys. Rev. C* **71**, 044616 (2005).